

# Damage detection monitoring applications in self-healing concrete structures using embedded piezoelectric transducers and recovery

G Karaiskos<sup>1,4</sup>, E Tsangouri<sup>1,2</sup>, D G Aggelis<sup>1</sup>, A Deraemaeker<sup>3</sup> and D Van Hemelrijck<sup>1</sup>

<sup>1</sup> Vrije Universiteit Brussels (VUB), Department Mechanics of Materials and Constructions (MeMC), Pleinlaan 2, B-1050, Brussels, Belgium

<sup>2</sup> SIM vzw-program SHE, Technologiemark 935, B-9052, Zwijnaarde, Belgium

<sup>3</sup> Université Libre de Bruxelles (ULB), Building, Architecture & Town Planning (BATir), 50 av F.D. Roosevelt, CP 194/02, B-1050, Brussels, Belgium

E-mail: [gkaraisk@vub.ac.be](mailto:gkaraisk@vub.ac.be)

**Abstract.** The ageing, operational and ambient loadings have a great impact in the operational and maintenance cost of concrete structures. Their service life prolongation is of utmost importance and this can be efficiently achieved by using reliable and low-cost monitoring and self-healing techniques. In the present study, the ultrasonic pulse velocity (UPV) method using embedded small-size and low-cost piezoelectric PZT (lead zirconate titanate) ceramic transducers in concrete with self-healing properties is implemented for monitoring not only the setting and hardening phases of concrete since casting time, but also for the detection of damage initiation, propagation and recovery of integrity after healing. A couple of small-scale notched unreinforced concrete beams are subjected to mode-I fracture through three-point bending tests. After a 24-hour healing agent curing period, the beams are reloaded using the same loading scenario. The results demonstrate the excellent performance of the proposed monitoring technique during the hydration, damage generation and recovery periods.

## 1. Introduction

Concrete is still the dominating structural material mainly due to its low production cost and the great structural design flexibility. Except the ageing, the concrete structures are vulnerable to a series of loadings such as ambient and operational. The monitoring, maintenance and renewal costs of the continuous ageing current concrete infrastructure are a major issue concerning a non-compromised prolongation of their operational service life. Reliable tools are required for error-free concrete strength and integrity performance evaluation, so that the most cost effective strategy of rehabilitation can be adopted. The main goal is to reduce the inspection costs and risks of unexpected failure not only in hardened state, but also during construction (setting and hardening phases) using real-time online monitoring systems [1].

<sup>4</sup> Author to whom any correspondence should be addressed.



Depending on the damage level caused, the monitoring techniques used for testing the structural integrity of concrete can be either destructive or non-destructive. Although the destructive methods provide generally direct, accurate and reliable structural assessment, these methods are harmful for the concrete structures. On the other hand, the non-destructive testing (NDT) methods indirectly evaluate the integrity of the structures. They mainly measure some other properties which can be correlated to compressive strength using an established relationship between the measured property and concrete strength. Moreover, the methods of concrete testing can be also divided into laboratory and in-situ applications. Until today, the mainstream way to inspect and test the integrity of concrete infrastructure with a high precision is a combination of destructive strength testing in a few samples coming from the existing structure as well as a thorough visual inspection of the whole structure. By definition, the aforementioned combination of monitoring techniques are extremely costly and time demanding, especially in the case of large-scale concrete facilities such as dams and tunnels, where a dense grid of measurement points is necessary. In the recent years, there is an increasing interest in NDT methods for both early-age and hardened concrete not only in the laboratory, but also in in-situ applications [2-5]. From cost and time points of view, the manual NDT inspection techniques are inefficient. Since the early 80's, the radical development in electronics and computer science have contributed a lot in the development of automated NDT structural health monitoring (SHM) for in-situ applications. The current trend is to use very large sensor networks which could be easily integrated in the design of the structures [6].

The ultrasonic pulse velocity (UPV) method has a major role among the various NDT methods in the field of SHM. It is one of the most reliable NDT methods for concrete early-age monitoring, strength estimation and damage detection. The majority of the commercially developed UPV systems are based on using bulky external piezoelectric transducers firmly held in contact with the surface of concrete and placed on two opposite faces of the tested structure (figure 1a). The testing system consists of a high voltage pulser, an amplifier and the main control unit. Because of the piezoelectric effect, the transducers can be used either as actuators (i.e. transmitters) or as sensors (i.e. receivers). A short-duration high-voltage pulse (500 to 1000 V) is introduced into the concrete through the transmitter. Then, longitudinal ultrasonic stress wave (i.e. *P*-wave) is generated and travels through the concrete. Finally, the *P*-wave is detected by the receiver which is placed at an opposite surface of the concrete at a distance  $L$ . A synchronized electronic timer, which is embedded in the main control unit, is responsible for measuring the transit time  $T$  of the *P*-wave traveling from the transmitter to the receiver. The transmitted pulses are subjected to loss and scattering because of the reflection, refraction and mode conversion caused by the aggregates, the possible voids and steel reinforcement possibly found along the travel path.

The longitudinal pulse velocity (in km/s or m/s) is simply calculated by dividing  $L$  by  $T$  and it could be correlated to the condition of the concrete [7].

$$V = \frac{L}{T} \quad (1)$$

The calculated velocity is directly related to the dynamic modulus of elasticity  $E$ , dynamic Poisson's ratio  $\mu$  and mass density  $\rho$  through the following equation [8].

$$V = \left( \frac{E(1-\mu)}{\rho(1+\mu)(1-2\mu)} \right)^{1/2} \quad (2)$$

It is obvious that the quality of the received signal depends on a series of parameters such as the accuracy of the measurement of the distance  $L$  as well as the quality of the coupling of the transducers to the concrete surfaces. Additionally, the necessity of placing the transducers in two opposite faces of the concrete structure, the lack of flexibility in the transducers arrangement as well as the lack of real-time online application make prohibitive the practical use of the technique.

One possible alternative of the bulky external transducers is to replace them by low-cost piezoelectric transducers which could be directly embedded inside the concrete (figure 1b). These

transducers were initially developed and applied in the University of Houston [9, 10]. Because of the stable coupling between the transducer and the concrete matrix the level of signal to noise ratio is quite higher than the one using the external transducers. They can be equally used for monitoring the hydration process of fresh concrete [11] as well as for SHM applications in hardened concrete [12].

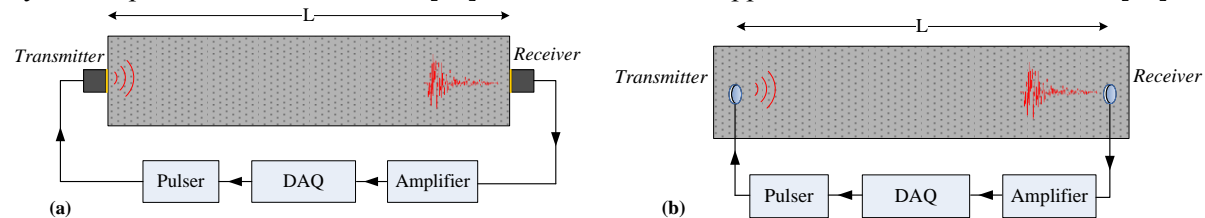


**Figure 1.** (a) Ordinary UPV test system and (b) UPV system based on small-size and low-cost embedded piezoelectric transducers.

Following the concept of ‘smart aggregates’ [9] (SMAG), a few transducers used in the present study were designed and fabricated in BATir at ULB. Each transducer consists of a low-cost flat piezoelectric PZT (lead zirconate titanate) small-dimension (12 mm x 12 mm x 0.2 mm) ceramic patch. The manufacturing steps of these transducers are shown in figure 2. Initially the cables are conductively glued with the patch (figure 2a-b). In order to avoid capacitive coupling interference between the transducers embedded in the fresh concrete (due to the presence of water) and to also mechanically protect it, the patch is properly insulated using a waterproof epoxy coating (figure 2c) and an extra electromagnetic protection is provided by applying a thin layer of conductive paint (figure 2d).

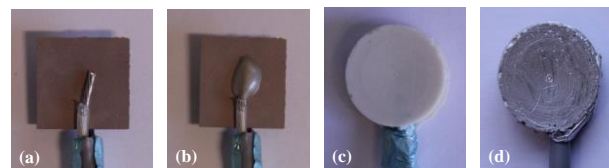


**Figure 2.** Manufacturing steps of the embedded transducers.

The current study is focused on the implementation of UPV method based on embedded low-cost piezoceramic transducers in a couple of small-scale notched unreinforced concrete beams with self-healing properties. Traditionally, the cracked concrete is manually healed by injecting epoxy and cement based agents into the gap of the cracks [13]. Here, the healing agent, which is filled within fragile small-dimension glass capsules, looks forward to self-healing the cracked concrete. One of the tested beams was monitored during setting and hardening period (hydration process) and both of them, after the hardening of concrete, were subjected to mode-I fracture through three-point bending tests. The beams were loaded until a wide crack opening and rupture of the capsules and release of the healing agent in the gap of the generated cracks were achieved. After a 24-hour curing period of the healing agent, the beams were reloaded using the same loading scenario. The performance of the proposed NDT technique for monitoring the concrete during the hydration period, the fracture process and fracture recovery is evaluated.

## 2. Experimental setup

A couple of small-scale (840 mm x 100 mm x 100 mm) notched unreinforced concrete beams with embedded self-healing system and low-cost piezoceramic transducers (SMAG–smart aggregate) were designed and manufactured in MeMC at VUB. The setup used in the experiments follows the Rilem Technical Report FMS-50 specifications [14]. The two-component expansive polyurethane-based

healing agent used in the present study was encapsulated in fragile small dimensioned glass capsules which were attached on very low stiffness plastic cord tightly fixed on the wooden mold (figure 3) [15]. In beam 1, two SMAGs (SMAG 1a and 1b) were embedded with a distance between them equal to 80 mm and at a height of 40 mm from the bottom of the beam. Additionally, four couples of short glass capsules (50 mm length, 3 mm diameter) filled with the two-component healing agent were symmetrically suspended at heights 35 mm and 60 mm from the bottom of the beam and a between distance of 50 mm on the same level. In beam 2, the monitoring system consisted of two couples of SMAGs which were embedded with a distance between them equal to 100 mm and at height levels equal to 38 mm (SMAGs 2a and 2b) and 63 mm (SMAGs 2c and 2d) from the bottom of the beam. Here, four couples of long glass capsules (75 mm length, 3 mm diameter) filled with the two-component healing agent were symmetrically suspended at heights 25 mm and 50 mm from the bottom of the beam and a distance between them equal to 50 mm on the same level.



**Figure 3.** Preparation of the beams with the self-healing system (glass capsules filled with healing agent) and the piezoceramic transducers (SMAGs).

After the concrete casting in the molds and until their demolding (three days later) both beams were subjected to membrane curing in order to prevent moisture loss. During that (early-age) period, the beam 1 was monitored by the UPV method based on the embedded piezoceramic transducers. Monitoring the transit time  $T$  needed by the transmitted  $P$ -waves to reach the receiver, it is feasible to estimate the mechanical properties of the concrete which can be related to parameters such as the percolation of solid particles and the degree of hydration. During that task, the SMAG-1a was the transmitter and the SMAG-1b was the receiver of the monitoring system. After demolding the beams and until their loading test (eleven days later), both of them were subjected to water curing in order to improve the setting and hardening procedure. Two weeks after the casting of concrete, both beams were subjected to mode-I fracture through three-point bending tests until a wide crack opening, rupture of the capsules and filling of the cracked area with the healing agent were achieved. Then the beams were unloaded and left in rest during the 24-hour curing period. Finally, the beams were subjected to the same loading tests in order to assess the monitoring and healing performance used in the current study. During loading and reloading tests, in beam 1 the SMAG-1a was the transmitter and the SMAG-1b was the receiver, as well as in beam 2 the SMAG-2a was the transmitter and the opposite placed SMAGs-2b, 2d were the receivers of the monitoring system (figure 6).

### 2.1. Early-age monitoring

In beam 1, after the concrete casting, high-voltage short-duration pulses (800 V / 2.5  $\mu$ s) were generated by the high voltage pulser and introduced into the concrete specimen through the transmitter (SMAG-1a). After traveling through the concrete, the generated  $P$ -waves were picked up by the receiver (SMAG-1b) whose signal was amplified. Initially and for the first 24 hours of the monitored early-age period, five tests every five minutes were performed and afterwards and until demolding the beam 1, five tests every twenty minutes were performed. By calculating the transit time  $T$  the wave takes to travel from the transmitter to the receiver, the wave velocity can be computed. In figure 4a, the evolution of the wave arrival time as a function of time during the monitored early-age period of beam 1 is shown. In the very early-age period (0-8 h) the signal to noise ratio of the received signals is very low and it was impossible to reliably compute the respective wave arrival time values. Using

equation (2) and assuming a dynamic Poisson's ratio equal to 0.3, the dynamic modulus of elasticity of the concrete during the same early-age is computed and its progression is shown in figure 4b.

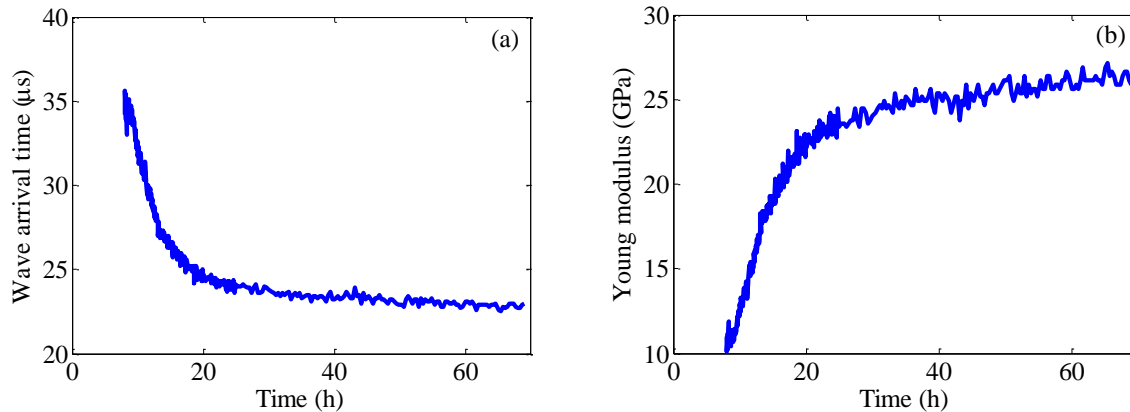


**Figure 4.** Evolution of the (a) wave arrival time and (b) dynamic modulus of elasticity as a function of time for beam 1.

By taking into account the time delay ( $2 \mu\text{s}$ ) of the transducers, computed through a calibration test before embedding them in the concrete and the distance between them ( $80 \text{ mm}$ ), the evolution of the  $P$ -wave velocity as a function of time for the monitored early-age period (figure 5) is easily calculated. A few recorded signals at different times are also shown in figure 5. It is obvious that the signal to noise ratio and the maximum amplitude of the recorded signals gradually increase and the transit time  $T$  is decreased during the transition from fluid to solid. The maximum amplitude of the recorded signals at very early-age period is however about one hundred times smaller than the one at an age of 60 h onwards.

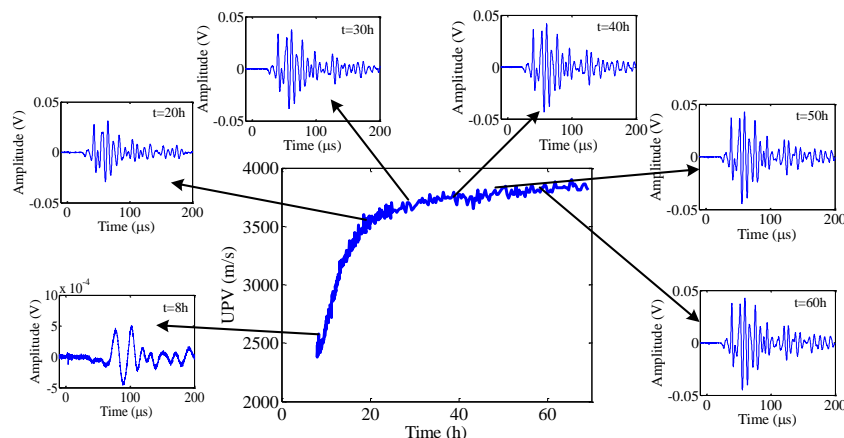


**Figure 5.** Evolution of the  $P$ -wave velocity as a function of time for beam 1.

## 2.2. Damage and healing monitoring

After a three-day membrane curing, both beams were demolded and subjected to water curing (submerged in a water bath) in order to improve the setting and hardening procedure until their loading test (eleven days later). Then, they were subjected to mode-I fracture through three-point bending tests under slow speed ( $0.04 \text{ mm/min}$ ) of the crosshead which was set in displacement control mode (figure 6). Following the loading rate, ten tests every fifteen seconds were performed and the mean value of each received group of results is used in the post processing of the results that follows. The loading is applied until a wide crack opening ( $0.3 \text{ mm}$ ), the rupture of the capsules and the filling of the cracked area with the healing agent were achieved. After unloading the beams, a 24-hour curing period of the

healing agent followed. Then, the beams were reloaded, following the same loading pattern, in order to assess the monitoring and healing performance used in the current study.

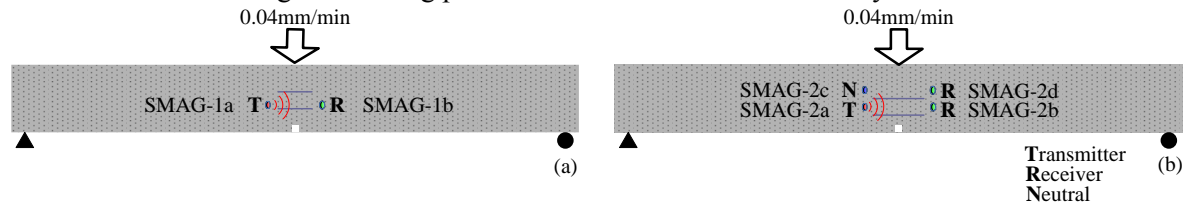


**Figure 6.** Experimental setup of the (a) beam 1 and (b) beam 2.

Due to the presence of aggregates and voids in the wave path between transmitter and receiver, the *P*-wave reaching the receiver was transformed into a complex waveform. The damage index used in the present study is based on the early part of that waveform and it considered both the shift of the arrival time as well as the amplitude of the received signals [12]. In figure 7a, the applied load (kN) vs strain (mm/mm) curves corresponding to the loading and reloading tests of beam 1 are shown. Load is the force applied by the crosshead of the testing machine used and strain is the normalized data (mm/mm) received by the crack mouth opening displacement (CMOD) gauge which was placed on the notch limits of the beam. Before testing, the initial opening of the gauge was fixed at 10 mm. Additionally, the gradual evolution of the early part of the recorded signals with increasing load corresponding to the loading test of beam 1 is shown in figure 7b.

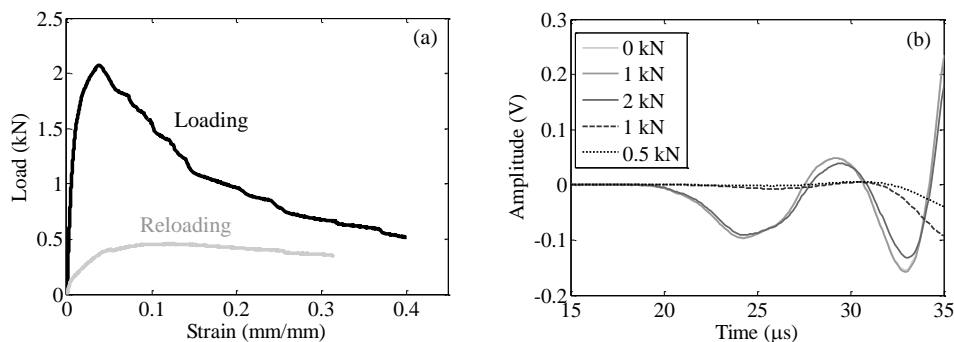


**Figure 7.** (a) Load vs strain (loading and reloading tests) and (b) evolution of the early part of the measured signals for beam 1 (loading test).

The change of the signals is well captured by the damage index for both beams in both tests as shown in figure 8, where its evolution is plotted as a function of the applied load.

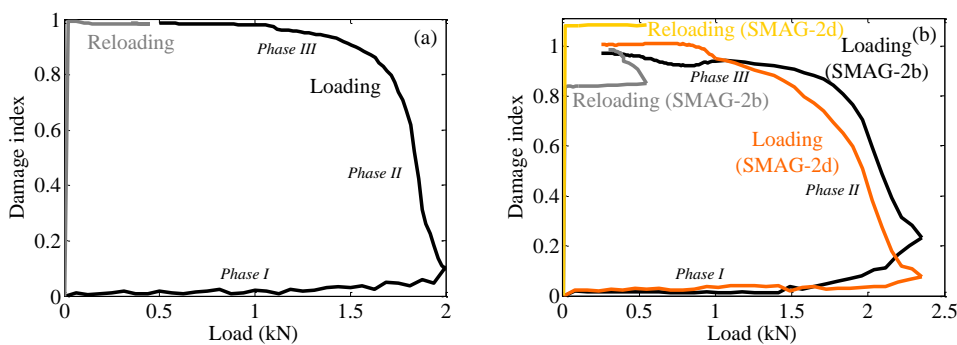


**Figure 8.** Damage index vs load for loading and reloading tests in (a) beam 1 and (b) beam 2.

In the loading tests, the damage index evolution graphs consist of three phases. The initiation (phase I) and progression (phase II) of the damage as well as the total failure (phase III) of the beams due to loading are clearly detected. In the first phase of loading tests in both beams, the damage index is very low but non-zero and this could be attributed to a certain level of noise in the received signals. The second phase corresponds to the initiation and evolution of damage (crack) in the concrete until the severe failure (third phase) where the damage index is almost unitary due to the fact that the wave cannot reach the receiver anymore. Additionally, in beam 2 and in the area between 1.5 kN and 2 kN, the damage index calculated by the results received by the lower embedded transducer (SMAG-2b) grows faster than the one by the higher placed transducer (SMAG-2d). This makes great sense as the crack initiates at the bottom of the beam 2, where the SMAG-2b is closely embedded. This is a solid indicator that the present UPV method cannot only efficiently detect the initiation of the damage, but also can track its evolution which makes it suitable for real-time online in-situ monitoring applications without giving a quantitative evaluation of the damage (size of crack). The damage index evolution graphs of the reloading tests, for both beams, consist of two parts. Initially, it is shown how the damage index evolves due to the curing process which is followed by the complete failure of the concrete. Unfortunately, in all the cases there is not any significant healing (recovery of mechanical properties) of the concrete due to the presence of the healing agent.

The recorded signals of beam 2 (SMAG-2b) in the end of the loading test and just before the reloading one are shown in figure 9. The presence of the dry healing agent has been well detected as in the signals before the reloading test, the arrival time has been decreased and the amplitude of the received signals has been increased.

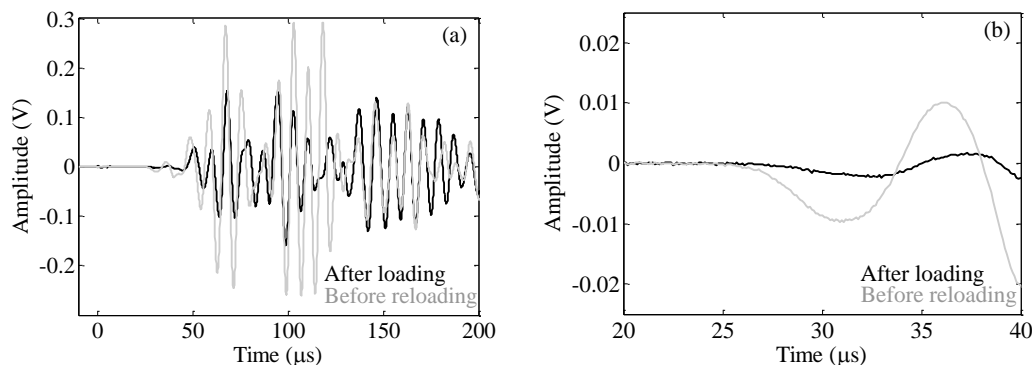


**Figure 9.** (a) Received signals by SMAG-2b (beam 2) after beam loading and before beam reloading and (b) the respective zooms in the early part of the graphs.

### 3. Conclusions and perspectives

Embedded piezoelectric transducers have been used for the monitoring of concrete with self-healing properties. Two small-scale notched unreinforced concrete beams with embedded self-healing system and low-cost piezoceramic transducers have been designed and manufactured. In one of the beams, the *P*-wave velocity has been monitored during the first three days after the concrete casting. After a two-week curing period, two three-point bending tests have been carried out on. The present monitoring technique is able not only to monitor the concrete structures during the setting and hardening period, but also to detect the initiation and follow the evolution of the cracking until complete failure of the structure. Even though the resulted performance of the self-healing technique used in the present study was not the desired one, the UPV method using embedded piezoelectric transducers was able to detect the presence of the healing agent. Next steps on the topic should be the quantitative assessment of damage using the received signals as well as the improvement of quality of the healing agent. The optimal placement of the capsules filled with the healing agent is a further topic that should be studied.

### Acknowledgements

The research described in this paper has been performed in the frame of the SIM program on Engineered Self-Healing Materials (SHE). The authors are grateful to SIM (Strategic Initiative Materials Flanders) and FNRS (Fonds de la Recherche Scientifique) for providing financial support.

### References

- [1] Bungey J H, Millard S G and Grantham M G 2006 *Testing of Concrete in Structures* (London and New York: Taylor & Francis)
- [2] ACI 228.2R-98 1998 Nondestructive test methods for evaluation of concrete in structures *American Concrete Institute*
- [3] ACI 228.1R-03 2003 In-place methods to estimate concrete strength *American Concrete Institute*
- [4] Popovics S 1998 *Strength and Related Properties of Concrete: A Quantitative Approach* (New York: John Wiley & Sons)
- [5] Malhorta V M and Carino N J 2004 *Handbook on Nondestructive Testing of Concrete* (Boca Raton: CRC Press)
- [6] Farrar C R and Worden K 2012 *Structural Health Monitoring: A Machine Learning Perspective* (New York: John Wiley & Sons)
- [7] ASTM C 597 – 67 1967 Standard test method for pulse velocity through concrete *American Society for Testing and Materials*
- [8] Krautkrämer J and Krautkrämer H 1969 *Ultrasonic Testing of Materials* (G. Allen & Unwin)
- [9] Gu H, Song G, Dhonde H, Mo Y L and Yan S 2006 Concrete early-age strength monitoring using embedded piezoelectric transducers *Smart Mater. Struct.* **15** 1837-45
- [10] Song G, Gu H, Mo Y L, Hsu T T C and Dhonde H 2007 Concrete structural health monitoring using embedded piezoceramic transducers *Smart Mater. Struct.* **16** 959-68
- [11] Dumoulin C, Karaiskos G, Carette J, Staquet S and Deraemaeker A 2012 Monitoring of the ultrasonic P-wave velocity in early-age concrete with embedded piezoelectric transducers, *Smart Mater. Struct.* **21** 047001
- [12] Karaiskos G, Flawinne S, Sener J Y and Deraemaeker A 2013 Design and validation of embedded piezoelectric transducers for damage detection applications in concrete structures *Proc. 10<sup>th</sup> Int. Conf. on Damage Assessment of Structures* (Trinity College Dublin, Ireland, 8-10 July 2013)
- [13] Smoak G 2002 *Guide to Concrete Repair* (New York: Books for Business)
- [14] RILEM TC-50-FCM 1985 Determination of fracture energy of mortar and concrete by means of three-point bend tests on notched beams *Mater. Struct.* **18** 285-90
- [15] Van Tittelboom K, De Belie N, Van Loo D, and Jacobs P 2011 Self-healing efficiency of cementitious materials containing tubular capsules filled with healing agent *Cement Concrete Comp.* **33** 497-505